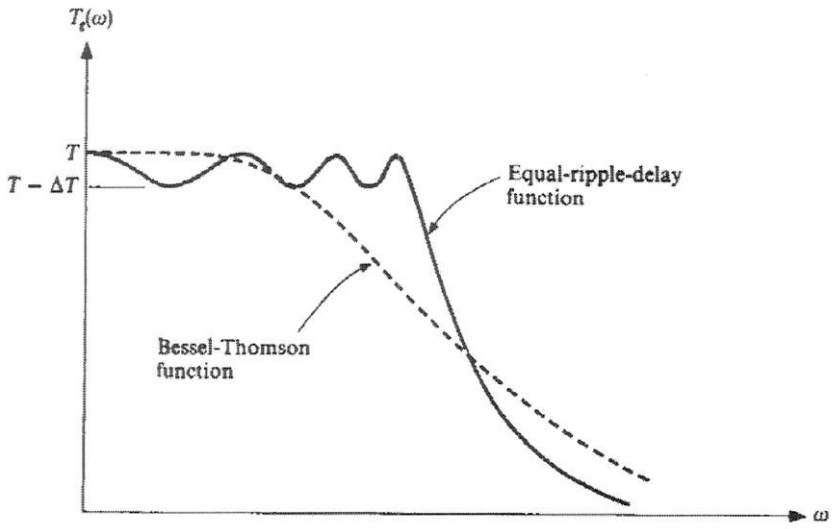

Figure 12-32 A comparison of the Bessel-Thomson and the equal-ripple delay functions.

troduced in Sec. 12-4; it is described in Ref. 11, which also contains an extensive tabulation of the corresponding natural modes. The derivation is straightforward but lengthy and hence is not included here; the reader should consult Ref. 3 for a discussion of the theory and Ref. 10 for the tables of natural modes. Reference 3 also contains a description of the rational function $H(s)$ which combines flat group delay in the passband with a Chebyshev loss in the stopband.

12-7 APPROXIMATION METHODS FOR BANDPASS FILTERS

Often the desired passband is not centered around the frequency origin but between two positive frequencies ω_{p_1} and ω_{p_2}, so that a bandpass rather than a low-pass filter is required. As discussed in Sec. 12-5, it is possible to design such a filter using a reactance transformation if the desired loss response has a geometric (logarithmic) symmetry around the band center frequency $\sqrt{\omega_{p_1}\omega_{p_2}}$. Also, a Moebius transformation can sometimes be used to obtain filter responses which are asymmetrical. Often, however, neither of these techniques is applicable, and the filter must be designed directly. In this section, therefore, a brief description will be given of direct approximation methods applicable for bandpass filters.

To obtain a bandpass loss response which is maximally flat at ω_0, we can use the function

$$|K(j\omega)|^2 = C_n \frac{(\omega^2 - \omega_0^2)^n}{\prod_{i=1}^{k} (\omega^2 - \omega_i^2)^2} \qquad K(s) = \pm C_n^{1/2} \frac{(s^2 + \omega_0^2)^{n/2}}{\prod_{i=1}^{k} (s^2 + \omega_i^2)} \quad (12\text{-}179)$$

where n is even and $k \leq n/2$. The characteristic function of (12-179) is clearly a modified version of that given in Eq. (12-36). It is easy to verify that $|K(j\omega)|^2$ and

its first $n-1$ derivatives with respect to ω^2 are all zero at $\omega = \pm\omega_0$, whatever the values chosen for the loss poles ω_i. An example of the loss response obtainable with this type of characteristic function is shown in Fig. 12-33. An iterative design process for finding the loss poles ω_i for prescribed α_p and specified minimum stopband loss is given in Ref. 2.

Equal-ripple passband general stopband bandpass filters can also be obtained by modifying the design technique described in Sec. 12-4. Now the transformation

$$Z \triangleq \sqrt{\frac{S^2+1}{S^2+\Omega_{p_1}^2}} = \sqrt{\frac{1+S^{-2}}{1+\Omega_{p_1}^2 S^{-2}}} \qquad \text{Re } Z \geq 0 \qquad (12\text{-}180)$$

is used to obtain the frequency-normalized response type illustrated in Fig. 12-34*a*. Following the discussion of Sec. 12-4, it can again be shown that the transformation of (12-180) maps the passband (which here extends from Ω_{p_1} to 1) to the jY axis. The upper stopband is mapped to $X_{s_2} \leq X \leq 1$, where X_{s_2} is the transformed value of Ω_{s_2}; the lower stopband is mapped to $1/\Omega_{p_1} \leq X \leq X_{s_1}$, where X_{s_1} is the transformed value of the lower stopband limit Ω_{s_1}. When $P(Z)$ is defined, as in Sec. 12-4, by (12-78), and $|K|^2$ by (12-79), the derivation proving the equal-ripple-passband character of the loss remains valid.

The only change in the design procedure given in Sec. 12-4 is that now there are loss poles at $\Omega = 0$, which contribute factors of the form $Z + 1/\Omega_{p_1}$ to the expression of $P(Z)$ given in (12-87). Hence, (12-87) is replaced by

$$P(Z) = \prod_{i=1}^{n} (Z + X_i) = \left(Z + \frac{1}{\Omega_{p_1}}\right)^{n_0} (Z+1)^{n_\infty} \prod_{i=1}^{(n-n_0-n_\infty)/2} (Z + X_i)^2 \qquad (12\text{-}181)$$

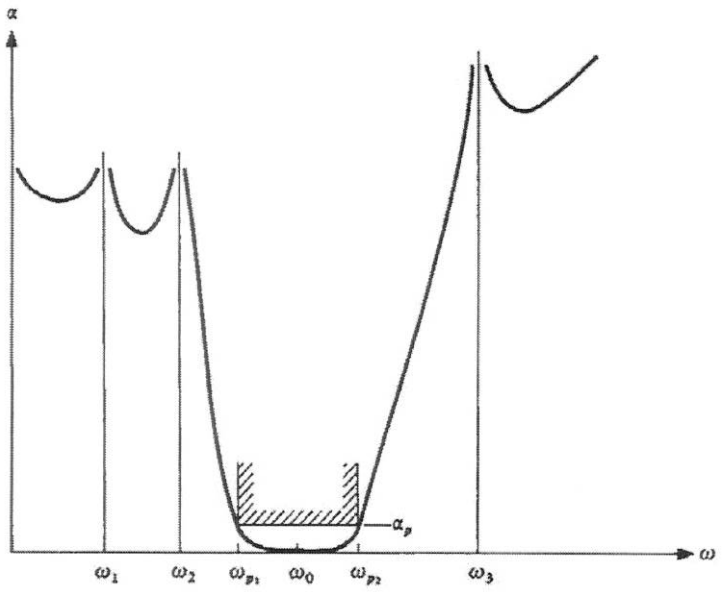

Figure 12-33 Maximally flat loss bandpass filter response.

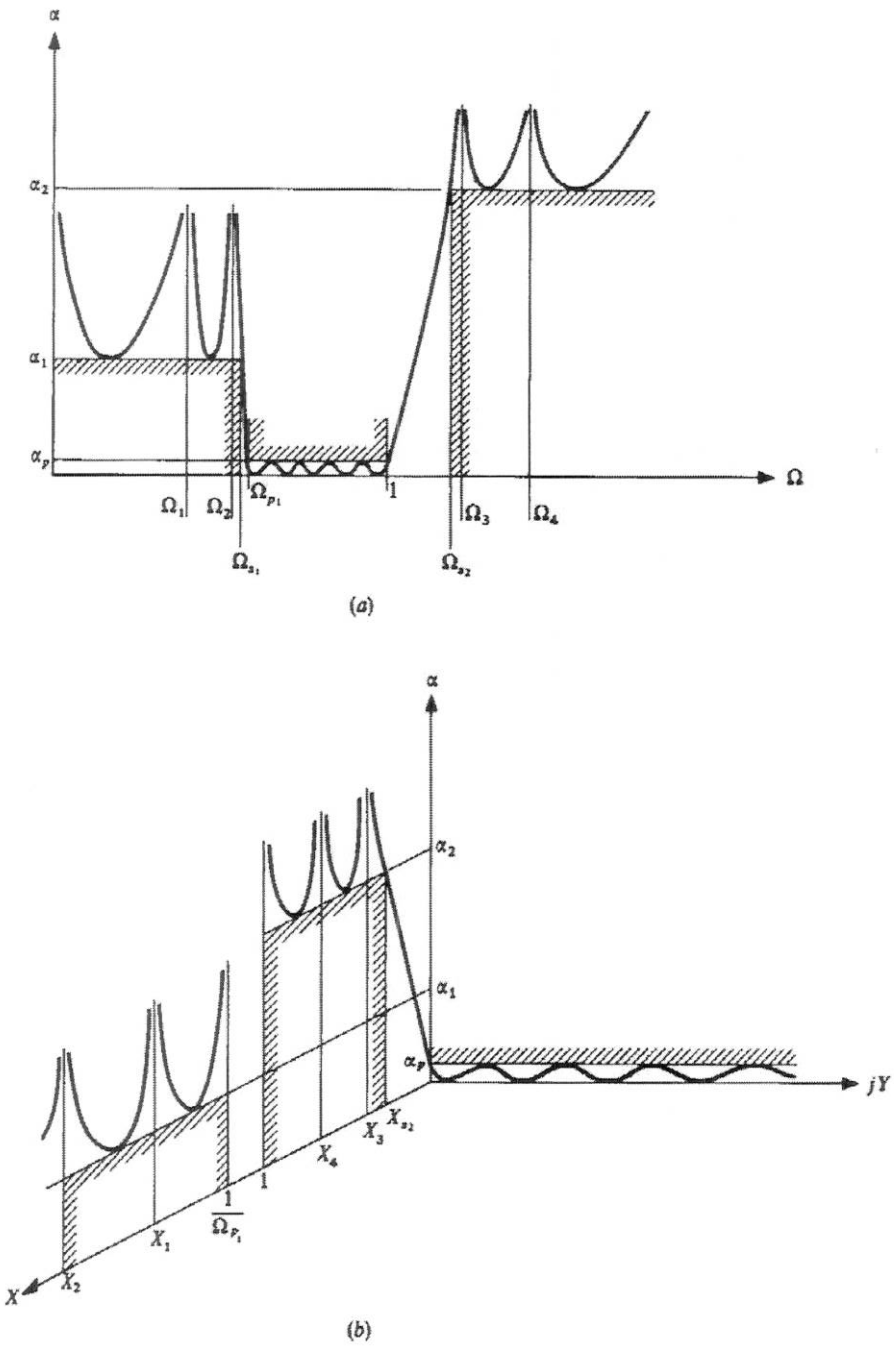

Figure 12-34 (*a*) Equal-ripple passband general stopband bandpass loss response; (*b*) loss response transformed into the Z plane.

where n_0 is the number of loss poles at $\Omega = 0$. Substituting into (12-79) gives

$$|K|^2 = k_p^2 \frac{[P_e(Z)]^2}{(-Z^2 + \Omega_{p_1}^{-2})^{n_0}(-Z^2+1)^{n_\infty} \prod_{i=1}^{(n-n_0-n_\infty)/2} (-Z^2 + X_i^2)^2} \qquad (12\text{-}182)$$

Using (12-180), it is easily shown that

$$\Omega_{p_1}^{-2} - Z^2 = \frac{(1-\Omega_{p_1}^2)S^2}{\Omega_{p_1}^2(S^2+\Omega_{p_1}^2)}$$

$$1 - Z^2 = \frac{-(1-\Omega_{p_1}^2)}{S^2+\Omega_{p_1}^2} \tag{12-183}$$

$$X_i^2 - Z^2 = \frac{1-\Omega_{p_1}^2}{\Omega_{p_1}^2-\Omega_i^2}\frac{S^2+\Omega_i^2}{S^2+\Omega_{p_1}^2}$$

It follows that the denominator of $|K|^2$ in (12-182) equals

$$D(S) = C\frac{S^{2n_0}\prod_{i=1}^{(n-n_0-n_\infty)/2}(S^2+\Omega_i^2)^2}{(S^2+\Omega_{p_1}^2)^n} \tag{12-184}$$

where C is a constant. Unless n is *even*, $D(S)$ is not a full square and hence no real rational $K(s)$ can be found from (12-182). Since $n = n_0 + n_\infty + 2m$, where m is the number of finite nonzero loss poles for positive Ω, this indicates that $n_0 + n_\infty$ must be even if this approximation is used.†

It will be noted that for $\Omega_{p_1} = 0$ and $n_0 = 0$, all formulas and hence the whole design procedure simplify to the low-pass filter approximation described in Sec. 12-4.

Next, the design of maximally flat-delay bandpass filters will be briefly discussed. The "obvious" process of obtaining such a filter by applying the low-pass–to–bandpass transformation (12-97) to the maximally flat-delay function derived in Sec. 12-6 is, unfortunately, useless. This can be seen by noting that the desired bandpass phase response is linear; the low-pass response found in Sec. 12-6 is indeed a linear-phase one, but the transformation (12-97) distorts the frequency axis in a nonlinear manner, as Fig. 12-22*c* illustrates. Hence, a phase response linear in ω around $\omega = 0$ becomes nonlinear in ω' around ω_1 after the transformation.

An exact solution to the flat-delay problem is possible, both for maximally flat and equal-ripple delay response.[3,11,12] However, the necessary derivations are lengthy and hence are omitted. Instead, a simple if inexact procedure will be described for obtaining an approximately flat-delay bandpass filter function from a flat-delay low-pass prototype. Let the natural modes of the low-pass filter be those shown in Fig. 12-35*a*. If the s variable is scaled so that the bandwidth of the low-pass response becomes equal to that of the desired bandpass bandwidth, the zero pattern of Fig. 12-35*b* is obtained. This scaling can be accomplished if we replace s by $[(\omega'_{p_2} - \omega'_{p_1})/2\omega_p]s$ in the linear-phase low-pass response $H(s)$. Next,

† The reader is referred for a detailed discussion of the design process to Ref. 2, which also describes a modified technique for synthesizing filters with odd degrees.

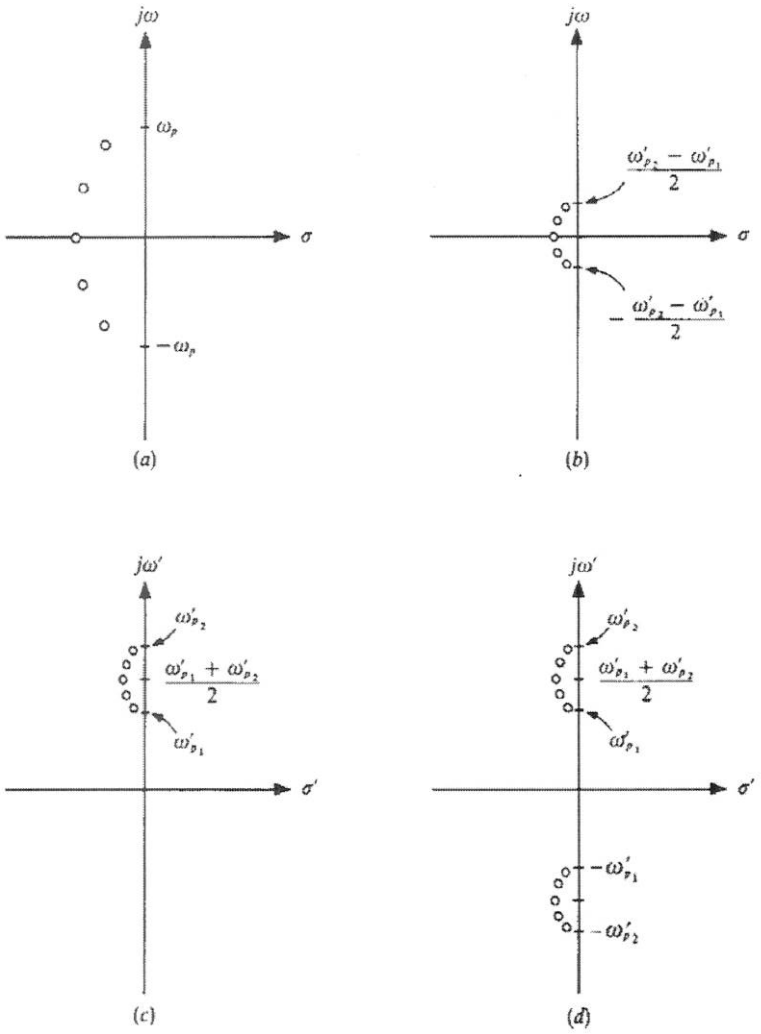

Figure 12-35 (*a*) Zero pattern for a flat-delay low-pass circuit; (*b*) scaled zero pattern; (*c*) scaled and shifted zero pattern; (*d*) realizable, approximately flat-delay bandpass zero pattern.

the zero pattern is *shifted* to the bandpass band center by adding $j(\omega'_{p_1} + \omega'_{p_2})/2$ to the scaled s variable (Fig. 12-35*c*). Thus, the new variable s' is given by

$$s' = \frac{\omega'_{p_2} - \omega'_{p_1}}{2\omega_p} s + j\frac{\omega'_{p_1} + \omega'_{p_2}}{2} \tag{12-185}$$

Solving for s and substituting into $H(s)$ gives the new response

$$H_1(s') = H(s) = H\left(\frac{2\omega_p}{\omega'_{p_2} - \omega'_{p_1}} s' - j\omega_p \frac{\omega'_{p_1} + \omega'_{p_2}}{\omega'_{p_2} - \omega'_{p_1}}\right) \tag{12-186}$$

Since all operations on s up to this point were linear, the new function $H_1(s')$ still possesses the linear-phase property. However, it is no longer realizable since it contains complex coefficients, as can be seen directly from (12-186) or from

Fig. 12-35*c*. To restore realizability, we must include the conjugates of all zeroes in the pattern, as indicated in Fig. 12-35*d*. The resulting transducer function

$$H_2(s') = H\left(\frac{2\omega_p}{\omega'_{p2} - \omega'_{p1}} s' - j\omega_p \frac{\omega'_{p1} + \omega'_{p2}}{\omega'_{p2} - \omega'_{p1}}\right) \times H\left(\frac{2\omega_p}{\omega'_{p2} - \omega'_{p1}} s' + j\omega_p \frac{\omega'_{p1} + \omega'_{p2}}{\omega'_{p2} - \omega'_{p1}}\right) \qquad (12\text{-}187)$$

is now real and hence realizable. However, the arbitrary addition of the conjugate zero pattern in the lower half plane is going to disturb the flat-delay property of $H_1(s')$ somewhat. If the relative bandwidth is very narrow, i.e., if the bandwidth $(\omega'_{p2} - \omega'_{p1})$ is much smaller than the band-center frequency $(\omega'_{p1} + \omega'_{p2})/2$, then the upper-half-plane zeros will be much closer to the passband portion $\omega'_{p1} \leq \omega' \leq \omega'_{p2}$ of the $j\omega'$ axis than the lower-half-plane zeros. Hence, for $(\omega'_{p2} - \omega'_{p1})/(\omega'_{p1} + \omega'_{p2}) \ll \frac{1}{2}$, the flat-delay property will be, to a good approximation, retained.

It should be noted that the transformation (12-187) from $H(s)$ to $H_2(s')$ alters the minimum absolute value of the function along the $j\omega$ axis. Hence, $|H(j\omega)| \geq 1$ for all ω does not guarantee $|H_2(j\omega')| \geq 1$ for all ω. Therefore, in general, a constant scaling factor C must also be included in $H^2(s')$.

The design process will be illustrated by a simple example.

Example 12-12 Find a transducer function $H_2(s')$ such that the specifications

$$T_g(\omega') = 0.5 \pm 0.05\ \mu s \qquad \alpha(\omega') \leq 1\ \text{dB}$$

are met in the frequency range 9.8 MHz $\leq f' \leq$ 10.2 MHz.

Since here the narrow-band condition $(\omega'_{p2} - \omega'_{p1})/(\omega'_{p1} + \omega'_{p2}) = 2\pi 0.4/2\pi 20 = 0.02 \ll \frac{1}{2}$ holds, the approximation of Eqs. (12-185) to (12-187) can be used. We can scale the time variable such that the required T_g becomes equal to 1 for the low-pass prototype function. This will enable us to use the results of Sec. 12-6 in the calculation of the prototype function. By Sec. 1-4, scaling the time by $T_g = 0.5\ \mu s$ is equivalent to scaling the radian frequency by $\omega_0 = 1/T_g = 2.0$ Mrad/s. By (12-185), $\omega_0 = (\omega'_{p2} - \omega'_{p1})/2\omega_p$, and hence the passband limit of the low-pass prototype is given by

$$\omega_p = \frac{\omega'_{p2} - \omega'_{p1}}{2\omega_0} = \tfrac{1}{2}(\omega'_{p2} - \omega'_{p1})T_g \approx 0.6283185$$

Since a 1-dB loss corresponds to a voltage ratio of about 0.89125, it is easy to establish from Figs. 12-30 and 12-31 that $n = 2$ barely meets the specifications. In order to allow for the distortion of the loss and delay responses inherent in this approximating process, we choose $n = 3$. Then, from Table 12-9,

$$H(s) = E^3(s) = s^3 + 6s^2 + 15s + 15$$

Next, we use (12-187) to obtain the bandpass function. After we define

$$\omega_1 = \omega_p \frac{\omega'_{p1} + \omega'_{p2}}{\omega'_{p2} - \omega'_{p1}}$$

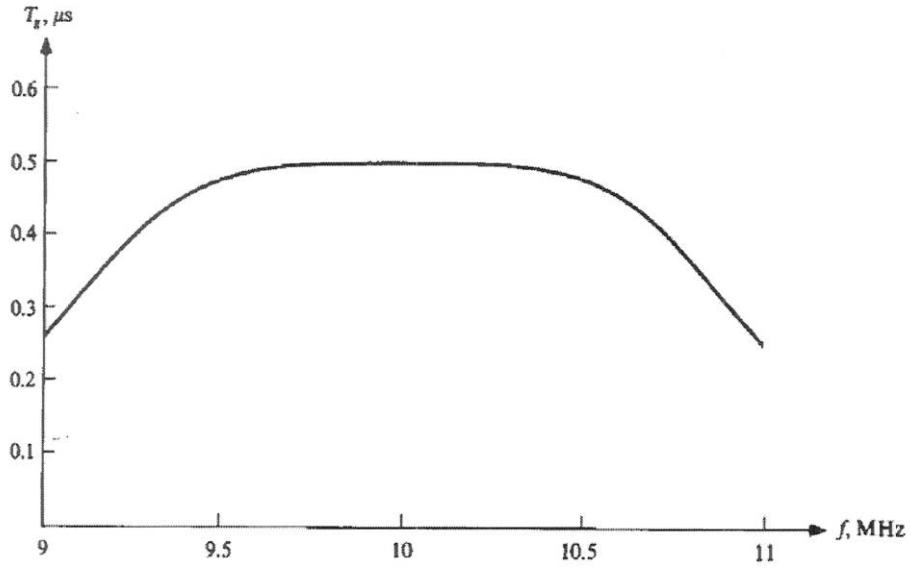

Figure 12-36 Group-delay response of a flat-delay bandpass filter.

(12-187) leads to

$$H_2(s') = H\left(\frac{s'}{\omega_0} - j\omega_1\right) H\left(\frac{s'}{\omega_0} + j\omega_1\right)$$
$$= C(s'^6 + a'_5 s'^5 + a'_4 s'^4 + a'_3 s'^3 + a'_2 s'^2 + a'_1 s' + a'_0)$$

Here, calculation gives

$$a'_5 = 2.4 \times 10^7 \qquad a'_4 \approx 1.210753 \times 10^{16}$$
$$a'_3 \approx 1.911765 \times 10^{23} \qquad a'_2 \approx 4.789984 \times 10^{31}$$
$$a'_1 \approx 3.76908 \times 10^{38} \qquad a'_0 \approx 6.1905886 \times 10^{46}$$

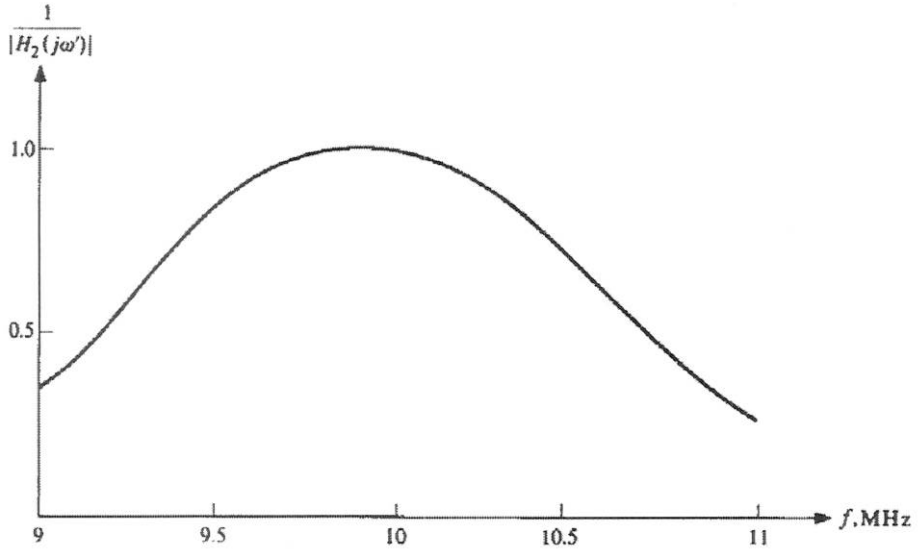

Figure 12-37 Amplitude response of a flat-delay bandpass filter.

The factor C can be found from the condition that the minimum value of $|H_2(j\omega')|$ must equal 1. This gives $C \approx 4.22011 \times 10^{-45}$.

The group-delay and amplitude responses corresponding to $H_2(j\omega')$ are shown in Figs. 12-36 and 12-37, respectively. All specifications are obviously met. In fact, the loss varies between 0 and 0.672 dB in the passband; the delay is between 0.50038 and 0.50081 μs.

Additional material pertaining to the solution of the approximation problem for bandpass filters can be found in Refs. 2, 3, and 11.

All discussions of this chapter have been carried out in terms of $H(s)$ and $K(s)$, that is, in terms of the parameters of a doubly terminated reactance two-port. These parameters satisfy the Feldtkeller equation $|H|^2 = 1 + |K|^2$ for $s = j\omega$, and hence $H(s)$ is subject to the restriction $|H(j\omega)| \geq 1$. For other types of circuits, e.g., active-RC filters, there may not exist any such limitation on the magnitude of the transfer function. Nevertheless, the derivations and results given in this chapter remain applicable, with a minor modification, which will be explained by example.

Example 12-13 To illustrate the process, assume that a third-degree active low-pass filter is to be designed with maximally flat-loss response. Let the desired voltage gain at zero frequency be $A_v(0) = 10$. Then we can introduce $H(s)$ through the relation

$$A_v(s) = \frac{A_v(0)}{H(s)} \tag{12-188}$$

Since $|A_v(j\omega)|$ has its maximum value at $\omega = 0$, the function $H(s)$ in (12-188) satisfies $|H(j\omega)| \geq 1$, just as before. Hence, we can use the Butterworth function obtained in Sec. 12-2 and tabulated in Table 12-2. This gives

$$A_v(s) = \frac{10}{s^3 + 2s^2 + 2s + 1}$$

which has all required properties.

It should also be pointed out that the whole of this chapter has been devoted to the approximation of prescribed *frequency* responses. Approximation of a prescribed *time* response is also possible. This subject is, however, beyond the scope of this book. The interested reader should consult Refs. 4 and 13.

12-8 SUMMARY

In this chapter, analytical methods were described for finding realizable network functions. They were applicable to lumped linear circuits, active or passive. The main emphasis was on filter transfer functions: low-pass, high-pass, and bandpass characteristics were considered in detail. The topics discussed included:

Bandpass design:
1. Transform from LPF:
a. reactance transf
b. Moebius transformation
2. Direct design
3. buffered
LPF HPF
4. Narrowba BPFs

Simpler, but restricted $f_{pi}, f_{si}; \alpha_s$

etically realizable) are too widely spread for easy practical construction; the ratios L_2'/l and C_1'/C_2' are over 130.

It is known from experience that this phenomenon is often encountered for *narro band* bandpass filters, i.e., for filters where $\omega'_{p1} - \omega'_{p2} \ll \sqrt{\omega'_{p1}\omega'_{p2}}$, as is the case here. T remedy the situation, the circuit equivalence shown in Fig. 12-24 may be used. The circu shown are equivalent if the following relations hold:

$$L_1' = L_1\frac{1-y}{2} \qquad C_1' = C_2 x\frac{1-z}{2} \tag{12-11}$$

$$L_2' = L_1\frac{1+y}{2} \qquad C_2' = C_2 x\frac{1+z}{2}$$

where

$$x \triangleq \left(1+\frac{C_1}{C_2}+\frac{L_2}{L_1}\right)^2 - 4\frac{C_1}{C_2}\frac{L_2}{L_1} \tag{12-11}$$

$$y \triangleq \sqrt{1-\frac{4L_2}{xL_1}} \qquad z \triangleq \sqrt{1-\frac{4C_1}{xC_2}}$$

For the circuit of Fig. 12-23*b*, $C_1/C_2 = L_2/L_1$ and hence (12-115) gives

$$x = 44.0291 \qquad y = z = 0.15102$$

Hence, using (12-114) and denormalizing the impedance level, i.e., multiplying all indu tances and dividing all capacitances by $R_0 = 150\ \Omega$, gives the element values indicated Fig. 12-23*c*. The spread of element values is now less than 7.

Next, consider the frequency transformation

$$\omega = A\frac{\omega'}{\omega_1^2 - \omega'^2} \tag{12-11}$$

Proceeding as we did before with (12-97), we can readily derive the correspondir element transformations (Fig. 12-25*a* and *b*) and the ω-vs.-ω' curve (Fig. 12-25*c* The latter makes it obvious that Eq. (12-116) transforms a low-pass filter into bandstop one. Figure 12-25*d* illustrates (for a Chebyshev filter) the resulting ma ping of the loss response.

HW

Since the analysis of this transformation is a close parallel of that of tl lowpass-to-bandpass transformation, the detailed calculations are left to tl reader as an exercise (see Probs. 12-31 to 12-34).

A review of Eqs. (12-91), (12-97), and (12-116) reveals that each of the relations replaces ω by a *reactance function* $f(\omega')$ of ω'. This makes it possible replace the immittances ωL_i and ωC_i of the lowpass prototype filter, one by on by realizable reactances to obtain the final high-pass (or bandpass or bandsto filter. Clearly this process can be generalized to more complicated reactance fun tions; however, the symmetry conditions which result become very complicat

Figure 12-25 (*a*) and (*b*) The transformation of low-pass prototype elements into bandstop fil impedances; (*c*) the transformation of the frequency variable; (*d*) the effect of the transformation the loss response.